Published in final edited form as:
Dev Biol. 2012 August 15; 368(2): 404–414. doi:10.1016/j.ydbio.2012.06.011.

mig-38, a novel gene that regulates distal tip cell turning during gonadogenesis in *C. elegans* hermaphrodites

Maria Martynovsky[a], **Ming-Ching Wong**[a], **Dana T. Byrd**[b], **Judith Kimble**[b], and **Jean E. Schwarzbauer**[a,*]

[a]Department of Molecular Biology, Princeton University, Princeton, NJ 08544 1014, USA

[b]Department of Biochemistry and Howard Hughes Medical Institute, University of Wisconsin-Madison, 433 Babcock Drive, Madison, WI 53706 1544, USA

Abstract

In *Caenorhabditis elegans* gonad morphogenesis, the final U-shapes of the two hermaphrodite gonad arms are determined by migration of the distal tip cells (DTCs). These somatic cells migrate in opposite directions on the ventral basement membrane until specific extracellular cues induce turning from ventral to dorsal and then centripetally toward the midbody region on the dorsal basement membrane. To dissect the mechanism of DTC turning, we examined the role of a novel gene, *F40F11.2/mig-38*, whose depletion by RNAi results in failure of DTC turning so that DTCs continue their migration away from the midbody region. *mig-38* is expressed in the gonad primordium, and expression continues throughout DTC migration where it acts cell-autonomously to control DTC turning. RNAi depletion of both *mig-38* and *ina-1*, which encodes an integrin adhesion receptor, enhanced the loss of turning phenotype indicating a genetic interaction between these genes. Furthermore, the integrin-associated protein MIG-15/Nck-interacting kinase (NIK) works with MIG-38 to direct DTC turning as shown by *mig-38* RNAi with the *mig-15*(*rh80*) hypomorph. These results indicate that MIG-38 enhances the role of MIG-15 in integrin-dependent DTC turning. Knockdown of talin, a protein that is important for integrin activation, causes the DTCs to stop migration prematurely. When both talin and MIG-38 were depleted by RNAi treatment, the premature stop phenotype was suppressed. This suppression effect was reversed upon additional depletion of MIG-15 or its binding partner NCK-1. These results suggest that both talin and the MIG-15/NCK-1 complex promote DTC motility and that MIG-38 may act as a negative regulator of the complex. We propose a model to explain the dual role of MIG-38 in motility and turning.

Keywords

Cell migration; Distal tip cell; *C. elegans*; Hermaphrodite gonadogenesis; *mig-38*; Integrin

Introduction

Cell migration is essential in many biological processes that are common among multicellular organisms including embryonic development, tissue morphogenesis, wound healing, and tissue homeostasis. Defects in regulation of cell migration contribute to many diseases and disorders such as arrested embryogenesis or cancer cell invasion and

*Corresponding author. Fax: +1 609 258 1035. jschwarz@princeton.edu (J.E. Schwarzbauer).

Appendix A. Supporting information: Supplementary data associated with this article can be found in the online version at http://dx.doi.org/10.1016/j.ydbio.2012.06.011.

metastasis. Gonadogenesis in the *Caenorhabditis elegans* hermaphrodite provides an excellent model for studying mechanisms governing cell migration. During this process two specialized somatic cells, called distal tip cells (DTC), undergo long-range migrations leading to the formation of U-shaped gonad arms (Hubbard and Greenstein, 2000; Lehmann, 2001). DTC migration is coordinated with progression through larval development (Hedgecock et al., 1987; Kimble and Hirsh, 1979; Kimble and White, 1981). The two DTCs are born from the Z1 and Z4 precursors in the middle of the first larval stage (L1) (Fig. 1). Migration begins in the second larval stage (L2), as the DTCs move along the ventral basement membrane of the body-wall muscles centrifugally away from the midbody. During the third larval stage (L3), DTCs turn away from the ventral side and migrate to the dorsal surface where they turn again and migrate centripetally toward the midbody region throughout the fourth larval stage (L4). DTC migration ceases opposite the vulva yielding fertile young adult hermaphrodites.

Several classes of evolutionarily conserved genes regulate DTC migration and pathfinding during different stages of the process (Cram et al., 2006; Lehmann, 2001; Nishiwaki, 1999). Initiation of migration requires the extracellular protease GON-1/ADAMTS (Blelloch et al., 1999) and a basement membrane protein PPN-1/MIG-6 (Cram et al., 2006; Kawano et al., 2009). Two integrin receptors mediate cell adhesion to the extracellular matrix in *C. elegans* (Gettner et al., 1995). One integrin heterodimer composed of INA-1/α and PAT-3/β subunits is expressed by the DTCs throughout migration and is required for movement (Baum and Garriga, 1997; Meighan and Schwarzbauer, 2007). The other integrin heterodimer (PAT-2/α; PAT-3/β) commences its expression at the time of DTC turning away from the ventral side and controls pathfinding (Lee et al., 2001; Meighan and Schwarzbauer, 2007). Cessation of DTC migration requires downregulation of INA-1/α integrin by a transcription factor VAB-3-dependent mechanism (Meighan and Schwarzbauer, 2007). The netrin receptor family regulates turning away from the ventral surface. The extracellular matrix protein UNC-6/netrin is expressed ventrally and its receptors in the DTCs, UNC-40 and UNC-5, mediate repulsion away from the ventral basement membrane (Hedgecock et al., 1990; Merz et al., 2001; Wadsworth et al., 1996).

Signaling pathways activated by integrins and netrin receptors regulate DTC motility and trajectory. Src tyrosine kinases are well-known mediators of integrin signaling (Playford and Schaller, 2004), and SRC-1 acts downstream of UNC-5 during DTC turning (Itoh et al., 2005; Lee et al., 2005a). Rac GTPases are involved in DTC migration (Reddien and Horvitz, 2000; Wu and Horvitz, 1998) in response to netrin (Lee et al., 2005a; Levy-Strumpf and Culotti, 2007) and integrin signaling (Lee et al., 2005b; Meighan and Schwarzbauer, 2007). Receptor-specific genes have also been identified such as talin, which is required for continuous movement and turning of the DTCs (Cram et al., 2003). Talin has an important role in stimulating integrin activity (Critchley, 2009; Shattil et al., 2010), and it provides a link to the cytoskeleton by binding to F-actin and actin-binding proteins (Critchley, 2009).

To identify other genes required for DTC migration, we carried out a genome-wide RNAi-based screen and identified 99 genes that caused significant defects in gonad morphogenesis (Cram et al., 2006). A small subset of these genes displayed a relatively rare RNAi phenotype, where, upon their downregulation, a dramatic defect in DTC turning was observed. This group includes factors previously established to have roles in cell migration, such as talin and *src-1*/Src kinase, as well as a novel gene, *F40F11.2/mig-38*. Knockdown of *mig-38* by RNAi disrupts turning of the DTCs resulting in the extension of the gonad arms away from the hermaphrodite midbody. Here we show that MIG-38 functions within DTCs and is required for execution of the DTC turn back toward the midbody region. We link this protein to integrin signaling and suggest a model to explain the role of MIG-38 in migration.

Materials and methods

C. elegans strains and RNAi

All *C. elegans* strains were maintained at 20 °C on NGM agar seeded with *Escherichia coli* OP50 (Hope, 1999). The N2 Bristol strain was used as wild type. The following strains used in this work were provided by the *Caenorhabditis* Genetics Center: wild-type N2, *rrf-3*(*pk1426*), *unc-6*(*ev400*), *mig-15*(*rh80*), *ina-1*(*gm144*). Strain NG2517, *gmIs5*[*ina-1*::*HGFP rol-6*(*su1006*)] is a translational fusion of GFP to intact *ina-1* including 5 kb of upstream sequence, able to rescue lethal allele *ina-1*(*gm86*) (Baum and Garriga, 1997). BC12753(*F40F11.2*p::GFP) was constructed by the British Columbia *C. elegans* Gene Expression Consortium and was obtained from the *Caenorhabditis* Genetics Center. To generate the DTC-specific RNAi strain, JK4143 [*qIs57 II; rde-1*(*ne219*) *V; qIs140*], we started with parental strain JK4135 [*qIs57; rde-1*(*ne219*)], where *qIs57* is a *lag-2*::GFP insertion (Siegfried et al., 2004) We injected JK4135 animals with *lag-2*p::RDE-1+pRF4 DNAs to create *qEx643*, an extrachromosomal array that was then integrated to create *qIs140*. The *rde-1* rescue of RNAi in the DTC was confirmed using GFP RNAi to reduce GFP expression.

The following RNAi clones used in this study were obtained from the *C. elegans* RNAi Library distributed by MRC geneservice courtesy of Julie Ahringer: *F40F11.2/mig-38*, *mig-15*, *ina-1*, *nck-1*, *pat-4*, and *talin*. The *src-1* RNAi clone was made by Erin Cram (Cram et al., 2006). We prepared *mig-38*^{JS1} and *mig-38*^{JS2} RNAi constructs by designing primers that target regions outside of 486–1574 (positions on the *F40F11.2b* cDNA relative to the ATG) in the Ahringer *F40F11.2* RNAi construct. Values in the primer names indicate the position on the cDNA relative to the ATG:

mig-38JS1: mig-38-2225–Forward: GCGAATTCCA TCGGAAATCGAA, and

mig-38-2460–Reverse: TGGAATTCGAGGAACCCTTA *mig-38JS2: mig-38*-2609–Forward: CAGAGCCAGAA CCGAAGAAG and

mig-38-3046–Reverse: TTGACTGGATTGCAGCTTTG.

These primers were used for PCR amplification from the cDNA template (prepared by RT-PCR of RNAs extracted from mixed stages of N2 nematodes). *Nhe*I and *Hind*III sites were added at the 5′ and 3′ ends, respectively, and were used to clone the PCR products into pPD129.36 vector. The RNAi feeding protocol used was essentially as described (Timmons, 2006). Briefly, bacteria carrying RNAi constructs in pPD129.36 were cultured overnight in LB liquid media supplemented with 40 μg/ml ampicillin, and then seeded onto NGM agar plates supplemented with IPTG (1 mM). For double and triple RNAi experiments, equal proportions of the cultured bacteria were seeded onto the plates. The expression of dsRNA was induced overnight at room temperature on the IPTG plates. Eggs were then transferred onto the plates and kept at 23 °C until the nematodes reached the desired stage of development.

Microscopy and sample preparation

To analyze gonad morphology, young adult or L4 hermaphrodites were mounted on a cover slip coated with 2% agarose in a drop of M9 buffer containing 0.08 M sodium azide and observed using a Nikon Diaphot 300 microscope equipped with DIC optics and a QImaging camera (QICAM). Anomalies such as migration in the wrong direction or migration without turning were scored as turning defects; aberrant stops were counted as defects in migration. Standard errors for the proportions of defective DTC migration and turning in a population were calculated using the observed frequency and sample size, assuming a binomial

distribution (http://www.statrek.com). Comparisons were done using a standard test (one-tailed for comparing two proportions).

To assess tissue expression of *F40F11.2/mig-38,* mixed-stage BC12753 (*F40F11.2*p::GFP) were immobilized on 2% agarose cover slips in 0.08 M sodium azide and viewed using PE RS3 Spinning Disk on Nikon T-2000 microscope equipped with the 100 × Plan Apo 1.4NA objective lens and a Hamamatsu ORIA ER-4 camera. Images were captured and managed using Volocity software. To visualize tissues underlying the muscles, gonads were dissected for imaging GFP in DTCs. Dissections were performed in PBS supplemented with 0.2 mM Levamisole. A 26G needle was used to decapitate the nematodes followed by evaluation of extruded gonad. Visualization was done using a Nikon Eclipse Ti microscope equipped for epifluorescence. Images were captured with a Hamamatsu ORCA R2 Camera using iVision software (BioVision technologies). Several images were tiled to reconstruct full-length organs and display morphological markers in Figs. 2–5.

Definition of phenotypes

Wild-type indicates the typical U-shaped gonad arm. “Wrong turn on dorsal” is the typical *mig-38* RNAi phenotype in which DTCs did not turn toward the midbody but continued to migrate away from the midbody on the dorsal side. “Extended linear” indicates a DTC that did not turn at all and continued to migrate on the ventral side. “Ventralized” describes the typical *unc-6*(*ev400*) phenotype in which the DTC did not make the ventral to dorsal turn but did turn toward the midbody on the ventral side.

In Tables 3 and 4, the phenotype categories are simplified. The “turn” category includes wrong turn on dorsal, extended linear, and extra turn (pathfinding) defects. The extra turn defects in which the DTC does not go back toward the midbody are also included in the wrong turn on dorsal category in Table 1 and Fig. 2C. The “short” category includes linear gonad arms that did not extend past the midpoint between the vulva and the end of the intestine and either remained on the ventral side or extended on the diagonal away from ventral.

Cloning of the F40F11.2 5′end

RNA from mixed-stage population nematodes was isolated. Briefly, nematodes were collected in M9 buffer. After dounce-homogenizing in 1 ml Trizol and β-mercaptoethanol (12.5 μl), the pellet was extracted twice using chloroform. RNA was precipitated using isopropanol, rinsed with ethanol, and resuspended in DEPC H_2O. RNA template (1 μg) was used to generate cDNA using Superscript reverse transcriptase primed with random hexamers. For PCR amplification 1 μl of the cDNA reaction was used as a template with these primers: SL1: 5′TTTAATTACCCAAGTTTGAG, F40F11.2RM: 5′ GTTGTACAGAAACGAATGTT. The 1500 bp amplicon was cloned into the T-vector (Promega) and sequenced.

Quantitative RT-PCR

The JE0164 *mwEx164* [*myo-3p*::*YFP*::*MIG-38*] transgenic strain (described in Supplementary Materials and Methods) was treated with *mig-38* or talin RNAi using the post-embryonic feeding protocol described above. Total RNA from RNAi-treated adult animals was isolated using TRIzol reagent (Life Technologies) and purified using the RNeasy Mini Kit (Qiagen). TRIzol was used according to manufacturer's instructions with the addition of a 5-min incubation in TRIzol reagent while vortexing the sample. RNA quantity was measured using a NanoDrop spectrophot-ometer (Thermo Scientific). 1 μg of total RNA per sample was reverse transcribed using SuperScript II Reverse Transcriptase (Life Technologies). The resulting cDNA was then used for realtime PCR analysis using

Brilliant II SYBR Green QPCR Master Mix with low ROX (Agilent Technologies) and a Stratagene Mx3000P QPCR system (Agilent Technologies). The following three reference genes were used as normalization factors for each cDNA sample: *pmp-3* (C54G10.3), *eif-3c* (T23D8.4), and Y45F10D.4, which encode a peroxisomal membrane protein, a eukaryotic initiation factor, and a putative iron–sulfur cluster assembly enzyme, respectively. These reference genes were chosen because they are not required for DTC migration (Cram et al., 2006) and have stable expression levels (Hoogewijs et al., 2008; Zhang et al., 2012). Primers were designed to produce an amplification product that spans an intron and does not overlap with the RNAi trigger sequences used for knockdown. Primer sequences are listed in Supplementary Table 1. Levels of *mig-38* or talin mRNA in RNAi-treated animals were compared to levels in RNAi control-treated animals. Based on the results of three independent experiments, JE0164 animals treated with *mig-38* RNAi exhibited a 24% decrease in mRNA levels (0.76 ± 0.07; $p < 0.01$), and those treated with talin RNAi exhibited a 69% decrease (0.31 ± 0.02; $p < 0.01$). Treated animals did not reproduce so we could not test expression in their offspring.

Results

F40F11.2/mig-38 acts cell-autonomously within DTCs to regulate their turning

The migration path of the DTCs during gonad morphogenesis is reflected in the final symmetrical U-shapes of the gonad arms (Fig. 1). The DTC trajectory is marked by two turns: the DTC re-orients away from the ventral basement membrane to migrate toward the dorsal side, and, once it reaches the dorsal surface, it turns to migrate toward the hermaphrodite midbody (Hedgecock et al., 1987). This gonad morphology is preserved in the *rrf-3*(*pk1426*) RNAi-sensitized nematodes (Simmer et al., 2003) when treated by feeding RNAi with bacteria carrying the pPD129.36 plasmid without an insert (Fig. 2A). Hermaphrodites subjected to post-embryonic *F40F11.2* RNAi have a distinctive abnormal gonad arm shape, demonstrating a defect in turning (Fig. 2B). 65±8% (N=145) of the DTCs fail to turn back toward the midbody region (Fig. 2C). Specificity of the RNAi phenotype was confirmed using constructs that target two other regions of the *F40F11.2* coding sequence. Treatment with these two constructs together gave 32 ± 9% of gonad arms (N= 100) with a wrong turn phenotype that was identical to the one produced by the original *F40F11.2* RNAi construct (Fig. 2C). Based on this DTC migration phenotype, this gene has been named *mig-38*.

During embryogenesis, *mig-38* plays an essential role since a deletion allele, *mig-38*(*ok2621*) (from the *C. elegans* Gene Knockout Consortium), has an embryonic lethal phenotype. Post-embryonic RNAi to knockdown *mig-38* expression allowed us to bypass this embryonic requirement. Off-target effects or variable phenotypic penetrance due to incomplete knockdown are caveats of the RNAi technique. As shown above, we tested multiple RNAi constructs that target different portions of the *mig-38* transcript, and all resulted in a consistent DTC migration phenotype. We have also conducted quantitative reverse transcription (qRT)-PCR for *mig-38* as well as for talin to show knockdown of expression in animals that have been treated with either *mig-38* or talin RNAi constructs, respectively (see Materials and Methods for details). Furthermore, genetic mutants, in addition to RNAi treatments, were used for parallel analysis whenever possible.

To determine whether *mig-38* functions cell-autonomously in DTCs, we depleted its expression with DTC-specific RNAi. JK4143 is a strain designed to restrict the RNAi machinery to DTCs. This strain is homozygous for *rde-1*(*ne219*) so that virtually all cells lack RDE-1, an Argonaute protein required for siRNA maturation (Yigit et al., 2006); however, it also carries a transgene harboring the wild-type *rde-1* gene under control of the *lag-2* promoter, which drives expression specifically in the DTCs in L3, L4 and adult

animals (Crittenden et al., 2006). When JK4143 hermaphrodites were treated with *mig-38* RNAi, 34 ± 8% (*N*= 122) of the gonad arms displayed a defect in DTC turning where the DTCs migrated away from the midbody on the dorsal basement membrane (Fig. 2C). The 34% defective gonad arms is significantly higher than in empty vector-treated *rde-1*(*ne219*); *lag-2p*::RDE-1 hermaphrodites [9 ± 5%, *N*= 105; $P \ll 0.001$]. These results show that *mig-38* acts cell-autonomously within the DTCs to regulate the turn toward the midbody.

MIG-38 is expressed by DTCs throughout migration

Two locations for the 5′ end of the *F40F11.2/mig-38* transcript are predicted in Wormbase; *F40F11.2*b lies 450 bp upstream of *F40F11.2*a. Using RT-PCR of RNAs prepared from mixed stages of N2 nematodes, we mapped the 5′ end to the *F40F11.2*b site which matches the position of GFP in the *F40F11.2*p::GFP transcriptional fusion construct generated by the BC *C. elegans* Gene Expression Consortium (Hunt-Newbury et al., 2007). In larvae and adult hermaphrodites, the *F40F11.2/mig-38* promoter-driven GFP signal is found mainly in neurons, muscles, and other contractile tissues such as the spermatheca (Hunt-Newbury et al., 2007). We detected *mig-38* expression in the somatic gonad precursors, Z1 and Z4 (Fig. 3A) and later within DTCs during larval and adult stages (Fig. 3B, C). Gonadal dissections allowed detection of *F40F11.2*p::GFP expression within the gonadal sheath cells (Fig. 3C and C′). However, expression was not observed in the germ cells or their precursors Z2 and Z3 (Fig. 3A and A′).

The *mig-38* gene is predicted to encode a relatively large 179 kD intracellular protein; no well-defined functional motifs have been identified in the protein sequence. MIG-38 is conserved among species of the *Caenorhabditis* genus. Hypothetical proteins homologous to MIG-38 are present in the genomes of *C. remanei* (CRE12805; 64% similarity), *C. japonica* (CJA12520; 62% similarity), *C. brenneri* (CBN13309; 62% similarity), and *C. briggsae* (CBG06120; 61% similarity). *Drosophila pseudoobscura* also contains a homologous hypothetical protein (GA28568; 25% similarity). One human protein, isoform F of proteoglycan 4 (ENSP00000356456; 28% similarity), shows homology over about half the length of MIG-38. A possible paralog of MIG-38 in *C. elegans* is DAO-5 (29% similarity), a predicted nucleolar protein. The unique nature of the MIG-38 sequence is intriguing given its importance in *C. elegans* gonadogenesis.

To provide insight into the subcellular localization of MIG-38, we generated a translational fusion of yellow fluorescent protein (YFP) to the *N*-terminus of MIG-38 under the control of the *myo-3* promoter. As a control, a transgenic strain that expresses YFP alone under the control of the *myo-3* promoter was generated. RT-PCR confirmed expression of the YFP::MIG-38 fusion transcript (Supplementary Fig. S1A). Fluorescence imaging of whole nema-todes showed YFP and YFP::MIG-38 in the cytoplasm of body wall muscle cells. YFP::MIG-38 also appeared to be localized in muscle cell nuclei (Supplementary Fig. S1B and C). Confocal microscopy of YFP localization in adult body wall muscles revealed that YFP::MIG-38 localizes to both the cytoplasm and the nucleus (Supplementary Fig. S2B–E). Compared to YFP localization (Supplementary Fig. 2A), YFP::MIG-38 localization appeared enriched in the nucleus (compare Supplementary Fig. S2A and A″ with B and B″). In analyses of at least 19 different nematodes from each strain, we observed nuclear enhancement in muscles from only 3% of *myo-3p*::YFP nematodes whereas 100% of *myo-3p*::YFP:: *MIG-38* muscles showed distinct nuclear localization as in Supplementary Fig. S2C–E. Imaging of live nematodes also showed enhanced nuclear expression (Supplementary Fig. 2F). These data indicate that MIG-38 localizes to both the cytoplasm and the nucleus, and therefore might have several distinct functions in regulating cell turning.

mig-38 acts during turning toward the midbody region

The majority of the gonad arms in *rrf-3*(*pk1426*) hermaphrodites treated with *mig-38* RNAi display a defect in DTC turning toward the midbody on the dorsal surface (Fig. 2C). To determine whether *mig-38* gene function is restricted to the dorsal side or whether it affects the turn toward the midbody independently of the dorsal location, we tested knockdown of *mig-38* in a ventralized *unc-6* mutant (Culotti and Merz, 1998; Hedgecock et al., 1990). *C. elegans* gene *unc-6* encodes a basement membrane protein UNC-6/netrin that serves as an extracellular guidance cue in many species (Ishii et al., 1992; Kennedy et al., 1994; Serafini et al., 1994). In *C. elegans*, UNC-6 expression is restricted to the ventral side where it induces turning of the DTC from ventral toward the dorsal side (Hedgecock et al., 1990; Wadsworth et al., 1996).

In *unc-6*(*ev400*) null mutants, DTC migration toward the dorsal side is compromised and DTCs remain on the ventral surface throughout all the stages of migration (Hedgecock et al., 1990; Wadsworth et al., 1996). In these mutants, the turn toward the midbody is executed by the DTCs on the ventral instead of the dorsal surface (Fig. 4A). This results in ventralized gonad arms, a phenotype characteristic of netrin mutants in late L4 and young adult stages [66 ± 8%, *N*=149] (Table 1). This defect was not observed in N2 wild-type hermaphrodites raised on an empty vector control or when treated with *mig-38* RNAi (Fig. 4B, Table 1). When *unc-6*(*ev400*) mutants were treated with *mig-38* RNAi, 62 ± 7% (*N*= 206) of the gonad arms were extended along the ventral side (Fig. 4C) indicating that the DTCs had not turned (Table 1). This extended linear phenotype was rarely observed in *unc-6*(*ev400*) mutants treated with an empty vector [5 ± 4%, *N*= 149] (Table 1), and it was not detected in wild-type N2 hermaphrodites treated with *mig-38* RNAi (Table 1). RNAi treatment is less effective in a wild-type background than in RNAi-sensitized *rrf-3*(*pk1426*) nematodes (Fig. 2C and Table 1). Even so, there was a dramatic increase in linearized gonad arms in *unc-6*(*ev400*) due to *mig-38* RNAi which shows that this phenotype represents a combined effect of the lack of UNC-6/netrin and reduction of MIG-38. Thus, *mig-38* acts within the DTCs to regulate the turn toward the midbody, and it has this effect whether the cells are positioned on the ventral or dorsal side of the animal. The high frequency of the extended linear gonad arm phenotype (62%) may suggest that the absence of netrin sensitizes *unc-6*(*ev400*) hermaphrodites to *mig-38* RNAi.

mig-38 interacts genetically with the ina-1 integrin adhesion receptor gene

The DTCs migrate along a basement membrane path during gonadogenesis and integrin receptors for extracellular matrix are required for this migration (Baum and Garriga, 1997; Lee et al., 2001; Meighan and Schwarzbauer, 2007). The INA-1/α integrin subunit pairs with the single β subunit encoded by the *pat-3* gene (Gettner et al., 1995). This heterodimer is expressed in DTCs and is required for their movement (Baum and Garriga, 1997; Meighan and Schwarzbauer, 2007). In the hypomorphic allele *ina-1*(*gm144*), with a missense mutation in the extracellular domain, DTC migration is misdirected on the dorsal surface (Baum and Garriga, 1997). Also, *ina-1* RNAi results in premature cessation of DTC migration (Meighan and Schwarzbauer, 2007). These phenotypes indicate that INA-1 is involved in regulating DTC migration and pathfinding.

To assess whether knockdown of expression of both *ina-1* and *mig-38* exacerbates the defects in turning, we treated *rrf-3*(*pk1426*) hermaphrodites and found a significant increase in the number of extended linear gonad arms [34 ± 8%, *N*=152] compared to animals treated with RNAi for *mig-38* [6 ± 3%, *N*=339; $P \ll 0.001$] or *ina-1* [7 ± 4%, *N*=132; $P \ll 0.001$] (Table 1). The increase in linear gonad arms shows an enhancement of the turning defect. The efficacy of *ina-1* RNAi was confirmed by treating NG2517 hermaphrodites expressing an INA-1::GFP translational fusion; we observed a GFP signal in 100% of DTCs when

treated with an empty vector (*N*= 40), but only 13% were fluorescent in *ina-1* RNAi-treated individuals (*N*= 39). We conclude that INA-1 integrins and MIG-38 act together to regulate DTC turning. With reduction of both gene products, the ability of DTCs to change the direction of migration is diminished.

mig-15/NIK contributes to integrin signaling during turning

In *C. elegans*, the *mig-15* gene encodes the ortholog of vertebrate Nck-interacting kinase (NIK) that binds to the PAT-3 integrin β subunit in vitro and functions in the *ina-1/pat-3* pathway to cell-autonomously regulate commissural axon navigation and motility (Poinat et al., 2002). To examine the connection between *mig-15* and *mig-38*, we compared their roles in DTC turning in hermaphrodites. Knockdown of *mig-15* expression affected DTC migration and induced the same wrong turn on the dorsal surface as observed with *mig-38* RNAi, albeit at much lower penetrance (Table 2). Hermaphrodites treated with *mig-15* RNAi displayed a small percentage of DTC turning defects [8 ± 4%, *N*= 146], where the cell migrates away from the midbody on the dorsal surface, a phenotype similar to *mig-38* RNAi. Knockdown of *mig-15* together with *mig-38* increased the total percentage of turning defects [49 ± 7%, *N*= 178] compared to either *mig-15* [8 ± 4%, *N*= 146; $P \ll 0.001$] or *mig-38* [30 ± 5%, *N*=278; $P \ll 0.001$] RNAi alone. The same DTC turning phenotype was observed in *mig-15*(*rh80*) hypomorphs (Table 2). This allele contains a premature stop codon after the kinase domain and is thus thought to retain partial MIG-15 activity (Shakir et al., 2006). 6 ± 3% of *mig-15*(*rh80*) DTCs did not execute the turn toward the midbody [*N*= 156], and this total percentage markedly increased upon treatment with *mig-38* RNAi [48 ± 14%, *N*= 52; $P \ll 0.001$] (Table 2). This rise in DTC turning defects is especially pronounced since, unlike *rrf-3*(*pk1426*), *mig-15*(*rh80*) hermaphrodites are not sensitized to RNAi, and *mig-38* RNAi only produced 14 ± 4% of DTC turning defects in the N2 background [*N*= 270; $P \ll 0.001$]. These results suggest that *mig-15* and *mig-38* act together to regulate DTC turning. Interestingly, we observed a dramatic increase in extended linear gonad arms upon reduction of *mig-38* expression in *mig-15*(*rh80*) hermaphrodites [33 ± 13%, *N*=52] compared to empty vector-treated *mig-15*(*rh80*) [3 ± 2%, *N*=156; $P \ll 0.001$]. A similar enhancement of the extended linear turning defect was also produced by *ina-1* and *mig-38* double RNAi, further suggesting that *mig-38* acts together with *mig-15* to regulate *ina-1* signaling during DTC turning.

mig-38 downregulation rescues DTC migration defects induced by talin RNAi

From our genome-wide screen, the small group of genes that affect turning back to the midbody region includes the gene encoding talin (Cram et al., 2003, 2006). Talin is a well-established activator of integrin receptors through its direct binding to the β integrin cytoplasmic domain (Pfaff et al., 1998; Shattil et al., 2010; Tadokoro et al., 2003; Wegener et al., 2007). Knockdown of *talin* by RNAi in wild-type hermaphrodites induces turning defects as well as early cessation of DTC migration (Cram et al., 2003).

Because of its direct link to integrins, we explored the relationship between talin and MIG-38 in DTC migration. Treatment of *rrf-3*(*pk1426*) hermaphrodites with *talin* RNAi resulted in defects in turning back to the midbody [37 ± 6%] and premature cessation of DTC migration producing short gonad arms [44 ± 7%, *N*=219] (Fig. 5A, Table 3) (Cram et al., 2003). A gonad arm was classified as “short” if the DTC stopped migrating at or before the midpoint between the vulva and the end of the intestine of the late L4/young adult hermaphrodite. The midpoint serves as a rough marker of the turning point for wild-type DTCs (Fig. 5C). Thus, premature cessation caused by *talin* RNAi occurs during DTC movement on the ventral side prior to the turn. In contrast to talin, knockdown of *mig-38* expression caused a defect in turning but not in forward movement (Table 3). In fact, the

malformed gonad arms extended well past the midpoint, and usually reached as far as the pharynx or the anus of a young adult hermaphrodite (see Fig. 2B).

Surprisingly, combined treatment of *rrf-3*(*pk1426*) hermaphrodites with *mig-38* and *talin* RNAi rescued the premature cessation of migration defect caused by *talin* RNAi (Fig. 5B). None of the gonad arms fit into the "short" category (Table 3) while there was a significant increase in the number of gonad arms that displayed defects in turning [82 ± 6%, *N*= 165] (Fig. 5C, Table 3). This latter effect indicates that talin was effectively downregulated in double RNAi treatment along with *mig-38*. Therefore, *mig-38* RNAi treatment suppresses the talin RNAi phenotype, which suggests that these two genes have opposing effects on DTC motility. Like *mig-38*, RNAi knockdown of *src-1* expression also caused defects in DTC turning [37 ± 9%, *N*= 102], but not in motility (Table 2). However, double knockdown of *src-1* with *talin* did not affect the percentage of short gonad arms [42 ± 9%, *N*= 104 compared to 44 ± 7%, *N*= 219] (Table 3), suggesting that suppression of this phenotype is specific to *mig-38*.

Measurements of the lengths of the gonad arms of hermaphrodites subjected to *talin* RNAi, *mig-38* RNAi, and *talin*, *mig-38* double RNAi confirmed the change in migration distance (Fig. 5C). Gonad arm length was normalized to the length of the intestine to account for differences in nematode size. We found that talin RNAi-treated animals had shorter gonad arms (median: 0.43, *N*= 29) than either double *mig-38*, *talin* RNAi-treated hermaphrodites (median: 0.77, *N*= 41) or *mig-38* RNAi treated animals (median: 0.99, *N*= 15). *mig-38* RNAi gonads with and without talin knockdown were consistently longer than the *talin* RNAi gonads (Fig. 5C). In contrast, the average gonad to intestine proportion in *src-1*, *talin* double RNAi-treated hermaphrodites (median: 0.47, *N*= 33) was similar to that of *talin* RNAi alone (median: 0.43, *N*= 29). These results support the conclusion that reduction of *mig-38* expression rescues the early DTC stopping defect caused by *talin* RNAi.

mig-15 and nck-1 have a role in DTC migration

Knockdown of *mig-38* expression compensates for the effects of talin depletion on DTC motility. However, both genes work with *ina-1*. Talin has a key function in activation of integrin receptors (Shattil et al., 2010), and we showed that *mig-38* and *ina-1* act together in DTC turning. One way for knockdown of mig-38 to promote migration in the absence of talin expression is by acting on integrins through a separate pathway from talin.

Since we found that MIG-38 works with MIG-15/NIK in turning, it seemed possible that these two proteins may also function in the regulation of DTC motility. A series of RNAi experiments with *rrf-3*(*pk1426*) or the *mig-15*(*rh80*) mutant was performed. In the triple RNAi treatments, nematodes were grown on plates with equal proportions of three bacterial strains carrying different RNAi constructs or the empty vector. As with double RNAi (Table 3), we again observed a significant reduction in short gonad arms in *rrf-3*(*pk1426*) hermaphrodites with knockdown of *mig-38* and *talin* [5.4 ± 3%, *N*= 280] compared to *talin* knockdown alone [51.5 ± 5%, *N*= 304]. Reduction of expression of *mig-15* along with *mig-38* and *talin* significantly increased the number of short gonad arms [22 ± 6%, *N*= 173 compared to 5.4 ± 3%; $P \ll 0.001$) (Table 4). Treatment of *mig-15*(*rh80*) hypomorphs with *mig-38* and *talin* double RNAi resulted in a similar percentage of short gonad arms [20 ± 7%, *N*= 144] as treatment with *talin* RNAi [compared with 28 ± 7%, *N*= 141]. Thus, *mig-38* RNAi does not suppress the motility defects from reduction of *talin* if *mig-15* is also reduced. These results suggest that, in contrast to the similar roles for *mig-38* and *mig-15* in DTC turning, in motility these genes have opposing roles. Interestingly, treatment of *mig-15*(*rh80*) hermaphrodites with *talin* RNAi resulted in a higher percentage of short gonad arms [28 ± 7%, *N*= 141] than *talin* RNAi treated N2 hermaphrodites [5 ± 3%, *N*= 152; $P \ll 0.001$] (Table 4), indicating that both MIG-15 and talin promote migration.

PAT-4/ILK is another integrin-associated protein (Mackinnon et al., 2002; Xu et al., 2006) and its downregulation by RNAi caused mild defects in DTC migration [3 ± 3%, *N*= 102] on the dorsal surface (Table 4). Unlike with *mig-15*, the premature stop of migration phenotype was not observed with triple knockdown of *pat-4*, *mig-38*, and *talin* [4 ± 4%, *N*= 99]; the percentage of occurrence was similar to *mig-38*, *talin*, *empty* RNAi [5.4 ± 3%, *N*= 280] (Table 4). Thus, reduction in *mig-15*, but not *pat-4*, can reverse *mig-38* RNAi suppression of migration defects that occur with depletion of talin.

MIG-15/NIK interacts with the Nck adapter protein, which also localizes to integrin adhesion sites (Buday et al., 2002; Li et al., 2001). The *C. elegans* ortholog of Nck is encoded by *nck-1*, which is required for migration of the excretory cells during excretory canal outgrowth (Schmidt et al., 2009). To determine whether *nck-1* regulates DTC migration and turning, we performed the same triple RNAi experiments as with *mig-15*; unlike *mig-15*, no suitable loss-of-function allele was available for *nck-1*. Knockdown of *nck-1* plus *talin* gave a small but significant increase in the percentage of short gonad arms [63 ± 9%, *N*=100] compared to *talin* RNAi [51.5 ± 5%, *N*=304; *P*=0.02] suggesting that both *nck-1* and *talin* genes act to promote motility. Triple RNAi with *nck-1*, *mig-38*, and *talin* gave a similar percentage of defects [20 ± 7%; *N*= 112] as with *mig-15*, *mig-38*, and *talin* RNAi treatment [22 ± 6%; *N*= 173] (Table 4). These results suggest similar roles for *nck-1* and *mig-15* in DTC motility and indicate that *mig-38* regulates a pathway containing both *mig-15* and *nck-1*.

Discussion

DTC migration is indispensible for gonadogenesis in *C. elegans* hermaphrodites. Multiple factors are involved in facilitating this process by driving motility and/or regulating pathfinding. One of the key events during DTC migration is a change in direction by cell turning. Wild-type DTCs execute a turn away from the ventral basement membrane toward dorsal, and then they turn on the dorsal basement membrane toward the midbody (Cram et al., 2006; Hedgecock et al., 1987; Nishiwaki, 1999). In this report, we have characterized *mig-38*, a gene that is required for execution of the turn toward the midbody. *mig-38* encodes a novel protein that acts in a DTC-autonomous manner to promote this turn on both the dorsal (as in wild-type) and ventral (as in the *unc-6*(*ev400*) ventralized mutant) surfaces. Our results link this protein to cell adhesion and motility. First, the turning defects are exacerbated with double knockdown of MIG-38 and either INA-1/α integrin or MIG-15/NIK, which binds to PAT-3/β integrin cytoplasmic domain (Poinat et al., 2002). Second, knockdown of *mig-38* expression restores DTC motility that is lost with talin RNAi. Since talin also interacts with integrin receptors (Pfaff et al., 1998; Tadokoro et al., 2003; Wegener et al., 2007), the suppressive effect when both genes are knocked down suggests that MIG-38 acts on DTC motility through a pathway that does not include talin.

The integrin heterodimer INA-1/PAT-3 has a major role in driving DTC motility (Baum and Garriga, 1997; Meighan and Schwarzbauer, 2007). This integrin is also involved in turning since simultaneous knockdown of *mig-38* and *ina-1* expression by RNAi significantly enhanced the penetrance of a no-turn, extended linear gonad arm phenotype. Turning defects were also observed with *mig-38* RNAi treatment of *ina-1*(*gm144*) hypomorphs, but the percentage of defects was not increased over RNAi treatment of wild type nematodes (unpublished observations). *ina-1*(*gm144*) has a missense mutation in the extracellular domain of the integrin that does not affect ligand binding, and the distinctive phenotype of this *ina-1* allele may result from interactions with two different extracellular ligands (Baum and Garriga, 1997). Proteins that act on the cytoplasmic tails of the integrins, as proposed for MIG-38, may not be able to modulate the effects of this extracellular mutation. Reduction of *mig-15*/NIK gene function produced the same turning defect as *mig-38* RNAi,

albeit with lower penetrance, and knockdown of both genes together significantly increased the number of turning defective gonad arms. Therefore, *mig-38* genetically interacts with *ina-1* and the associated kinase gene *mig-15* to regulate turning. We propose that MIG-38 acts through MIG-15 to affect the function of the INA-1/PAT-3 heterodimer in this process (Fig. 6A).

Talin promotes integrin activity by binding to the β integrin cytoplasmic domain (Pfaff et al., 1998; Shattil et al., 2010; Tadokoro et al., 2003; Wegener et al., 2007) and it also links integrins to the actin cytoskeleton (Critchley, 2009). Loss of talin had a similar effect on DTC turning as loss of MIG-38 (this report and (Cram et al., 2006), but talin is also required for DTC movement since reduction of its expression gave a significant proportion of short gonad arms. These effects on turning and motility suggest that talin binding to PAT-3/β integrin has a dual role in DTC migration. It is needed for forward motility so that when it is knocked down, the DTCs stop prematurely. For those cells that continue forward movement, talin is needed to change direction and, in its absence, the cells do not turn back toward the midbody region. Since talin binds directly to the β integrin cytoplasmic domain and stimulates integrin activity, the reduction-of-talin effects could result from reduced levels of integrin activity during movement and/or at the turn. Knockdown of talin expression will also change the connection between integrins and the actin cytoskeleton (Critchley, 2009; Shattil et al., 2010), which suggests that perturbation of cell shape changes may also contribute to the defects in motility and turning.

Our data show that reduction of talin expression causes a motility defect that is suppressed by MIG-38 depletion. This suggests that *mig-38* affects a motility-promoting pathway, but one that is separate from talin (Fig. 6B). Knockdown of MIG-15 or NCK-1 counteracted the suppressive effects of MIG-38 leading to an increase in short gonad arms, linking these molecules to cell motility. Vertebrate studies implicate MIG-15/NIK in regulating changes in cell morphology through phosphorylation of actin-modulating ERM proteins resulting in extension of lamellipodia (Baumgartner et al., 2006). Also, mammalian NIK regulates adhesion through promoting integrin activation downstream of Eph receptors (Becker et al., 2000). MIG-15/NIK is involved in cell movement and pathfinding of migrating neurons and neuroblasts in *C. elegans* (Chapman et al., 2008; Poinat et al., 2002; Shakir et al., 2006). This kinase also regulates development and maintenance of cell polarity in Q neuroblasts (Chapman et al., 2008). In a loss-of-function *mig-15*(*rh80*) mutant, more than one-third of the Q cells elaborated cell extensions in the wrong direction or failed to polarize at all (Chapman et al., 2008). Similar to these findings in neurons, our data point to a dual role for MIG-15/NIK in controlling motility and directionality of DTCs through integrins (Fig. 6A and B).

The binding partner of MIG-15/NIK, NCK-1/Nck adapter protein, serves as a link between cell surface receptors, including integrins, and the actin cytoskeleton (Buday et al., 2002; Li et al., 2001). Numerous signaling molecules bind to Nck in different cellular systems, and assessing the physiological importance of these interactions is a subject of active investigation (Buday et al., 2002; Funasaka et al., 2010; Lettau et al., 2009). Nck has been implicated in axon guidance and cell migration in flies (Buday et al., 2002), and our data link NCK-1 to cell motility since its loss increased the penetrance of the short gonad arm phenotype in the absence of talin. Therefore, we suggest that the MIG-15/NCK-1 complex is involved in promoting DTC motility (Fig. 6B).

Can we reconcile a synergistic role for MIG-38 with one integrin-associated protein, MIG-15, and an opposing role with another, talin? We propose that both MIG-15/NCK and talin contribute to motility through their interactions with PAT-3/β integrin (Fig. 6B). Our data suggest that *mig-38* negatively impacts the function of the MIG-15/NCK-1 complex

such that the reduction of both MIG-38 and talin allows this complex to substitute for talin and promote motility. The proposed inhibitory effect of a MIG-38 pathway on MIG-15/NCK-1 may promote dissociation of the complex, thus allowing MIG-15 to interact with other factors and participate in integrin-mediated turning (Fig. 6A). In this model, MIG-38 positively affects MIG-15 and its interaction with INA-1/PAT-3 integrin to promote a change in the direction of DTC migration (Fig. 6A). Given its apparent localization to both the cytoplasm and nucleus, MIG-38 could act directly on this pathway or indirectly perhaps through effects on gene expression. Thus when MIG-38 is depleted, stimulation of a turning pathway is reduced, but MIG-15 could still couple with NCK-1 and promote DTC motility.

Mechanistically, MIG-38 might function in turning through control of cell polarity. MIG-15/NIK has previously been shown to control the development of cell polarity (Chapman et al., 2008) and our findings show a synergistic effect between MIG-38 and MIG-15/NIK in turning raising the possibility that MIG-38 acts as a switch from forward movement to turning by invoking MIG-15 function in repolarization.

Supplementary Material

Refer to Web version on PubMed Central for supplementary material.

Acknowledgments

We thank Hongyu Shang for critical reading of the manuscript and valuable suggestions, Joe Goodhouse for his help with microscopy, R. Daniel Slone for technical help, and Andrew Fire (Stanford University, Stanford, CA) for the L4817 vector. Some nematode strains used in this work were provided by the *Caenorhabditis* Genetics Center, which is funded by the NIH National Center for Research Resources (NCRR). Funding was provided to JES by NIH R01GM059383 and by the Cell Migration Consortium GLUE Grant no. NIH U54 GM064346. MM was supported by the NIH pre-doctoral training Grant no. 5T32GM007388. MCW was a postdoctoral fellow of the New Jersey Commission on Cancer Research.

References

Baum PD, Garriga G. Neuronal migrations and axon fasciculation are disrupted in ina-1 integrin mutants. Neuron. 1997; 19:51–62. [PubMed: 9247263]

Baumgartner M, Sillman AL, Blackwood EM, Srivastava J, Madson N, Schilling JW, Wright JH, Barber DL. The Nck-interacting kinase phosphorylates ERM proteins for formation of lamellipodium by growth factors. Proc Natl Acad Sci USA. 2006; 103:13391–13396. [PubMed: 16938849]

Becker E, Huynh-Do U, Holland S, Pawson T, Daniel TO, Skolnik EY. Nck-interacting Ste20 kinase couples Eph receptors to c-Jun N-terminal kinase and integrin activation. Mol Cell Biol. 2000; 20:1537–1545. [PubMed: 10669731]

Blelloch R, Anna-Arriola SS, Gao D, Li Y, Hodgkin J, Kimble J. The gon-1 gene is required for gonadal morphogenesis in *Caenorhabditis elegans*. Dev Biol. 1999; 216:382–393. [PubMed: 10588887]

Buday L, Wunderlich L, Tamas P. The Nck family of adapter proteins: regulators of actin cytoskeleton. Cell Signalling. 2002; 14:723–731. [PubMed: 12034353]

Chapman JO, Li H, Lundquist EA. The MIG-15 NIK kinase acts cell-autonomously in neuroblast polarization and migration in *C. elegans*. Dev Biol. 2008; 324:245–257. [PubMed: 18840424]

Cram EJ, Clark SG, Schwarzbauer JE. Talin loss-of-function uncovers roles in cell contractility and migration in *C. elegans*. J Cell Sci. 2003; 116:3871–3878. [PubMed: 12915588]

Cram EJ, Shang H, Schwarzbauer JE. A systematic RNA interference screen reveals a cell migration gene network in*C. elegans*. J Cell Sci. 2006; 119:4811–4818. [PubMed: 17090602]

Critchley DR. Biochemical and structural properties of the integrinassociated cytoskeletal protein talin. Annu Rev Biophys. 2009; 38:235–254. [PubMed: 19416068]

Crittenden SL, Leonhard KA, Byrd DT, Kimble J. Cellular analyses of the mitotic region in the *Caenorhabditis elegans* adult germ line. Mol Biol Cell. 2006; 17:3051–3061. [PubMed: 16672375]

Culotti JG, Merz DC. DCC and netrins. Curr Opin Cell Biol. 1998; 10:609–613. [PubMed: 9818171]

Funasaka K, Ito S, Hasegawa H, Goldberg GS, Hirooka Y, Goto H, Hamaguchi M, Senga T. Cas utilizes Nck2 to activate Cdc42 and regulate cell polarization during cell migration in response to wound healing. FEBS J. 2010; 277:3502–3513. [PubMed: 20637038]

Gettner SN, Kenyon C, Reichardt LF. Characterization of beta pat-3 heterodimers, a family of essential integrin receptors in *C. elegans*. J Cell Biol. 1995; 129:1127–1141. [PubMed: 7744961]

Hedgecock EM, Culotti JG, Hall DH. The unc-5, unc-6, and unc-40 genes guide circumferential migrations of pioneer axons and mesodermal cells on the epidermis in *C. elegans*. Neuron. 1990; 4:61–85. [PubMed: 2310575]

Hedgecock EM, Culotti JG, Hall DH, Stern BD. Genetics of cell and axon migrations in *Caenorhabditis elegans*. Development. 1987; 100:365–382. [PubMed: 3308403]

Hoogewijs D, Houthoofd K, Matthijssens F, Vandesompele J, Vanfleteren JR. Selection and validation of a set of reliable reference genes for quantitative sod gene expression analysis in *C. elegans*. BMC Mol Biol. 2008; 9:9. [PubMed: 18211699]

Hope, IA. *C elegans*, A Practical Approach. Oxford University Press; Oxford: 1999.

Hubbard EJ, Greenstein D. The *Caenorhabditis elegans* gonad: a test tube for cell and developmental biology. Dev Dyn. 2000; 218:2–22. [PubMed: 10822256]

Hunt-Newbury R, Viveiros R, Johnsen R, Mah A, Anastas D, Fang L, Halfnight E, Lee D, Lin J, Lorch A, McKay S, Okada HM, Pan J, Schulz AK, Tu D, Wong K, Zhao Z, Alexeyenko A, Burglin T, Sonnhammer E, Schnabel R, Jones SJ, Marra MA, Baillie DL, Moerman DG. High-throughput in vivo analysis of gene expression in *Caenorhabditis elegans*. PLoS Biol. 2007; 5:237.

Ishii N, Wadsworth WG, Stern BD, Culotti JG, Hedgecock EM. UNC-6, a laminin-related protein, guides cell and pioneer axon migrations in *C. elegans*. Neuron. 1992; 9:873–881. [PubMed: 1329863]

Itoh B, Hirose T, Takata N, Nishiwaki K, Koga M, Ohshima Y, Okada M. SRC-1, a non-receptor type of protein tyrosine kinase, controls the direction of cell and growth cone migration in *C. elegans*. Development. 2005; 132:5161–5172. [PubMed: 16251208]

Kawano T, Zheng H, Merz DC, Kohara Y, Tamai KK, Nishiwaki K, Culotti JG. *C. elegans* mig-6 encodes papilin isoforms that affect distinct aspects of DTC migration, and interacts genetically with mig-17 and collagen IV. Development. 2009; 136:1433–1442. [PubMed: 19297413]

Kennedy TE, Serafini T, de la Torre JR, Tessier-Lavigne M. Netrins are diffusible chemotropic factors for commissural axons in the embryonic spinal cord. Cell. 1994; 78:425–435. [PubMed: 8062385]

Kimble J, Hirsh D. The postembryonic cell lineages of the hermaphrodite and male gonads in *Caenorhabditis elegans*. Dev Biol. 1979; 70:396–417. [PubMed: 478167]

Kimble JE, White JG. On the control of germ cell development in *Caenorhabditis elegans*. Dev Biol. 1981; 81:208–219. [PubMed: 7202837]

Lee J, Li W, Guan KL. SRC-1 mediates UNC-5 signaling in *Caenorhabditis elegans*. Mol Cell Biol. 2005a; 25:6485–6495. [PubMed: 16024786]

Lee M, Cram EJ, Shen B, Schwarzbauer JE. Roles for beta(pat-3) integrins in development and function of *Caenorhabditis elegans* muscles and gonads. J Biol Chem. 2001; 276:36404–36410. [PubMed: 11473126]

Lee M, Shen B, Schwarzbauer JE, Ahn J, Kwon J. Connections between integrins and Rac GTPase pathways control gonad formation and function in *C.elegans*. Biochim Biophys Acta. 2005b; 1723:248–255. [PubMed: 15716039]

Lehmann R. Cell migration in invertebrates: clues from border and distal tip cells. Curr Opin Genet Dev. 2001; 11:457–463. [PubMed: 11448633]

Lettau M, Pieper J, Janssen O. Nck adapter proteins: functional versatility in T cells. Cell Commun Signal. 2009; 7:1. [PubMed: 19187548]

Levy-Strumpf N, Culotti JG. VAB-8, UNC-73 and MIG-2 regulate axon polarity and cell migration functions of UNC-40 in *C. elegans*. Nat Neurosci. 2007; 10:161–168. [PubMed: 17237777]

Li W, Fan J, Woodley DT. Nck/Dock: an adapter between cell surface receptors and the actin cytoskeleton. Oncogene. 2001; 20:6403–6417. [PubMed: 11607841]

Mackinnon AC, Qadota H, Norman KR, Moerman DG, Williams BD. *C. elegans* PAT-4/ILK functions as an adapter protein within integrin adhesion complexes. Curr Biol. 2002; 12:787–797. [PubMed: 12015115]

Meighan CM, Schwarzbauer JE. Control of *C. elegans* hermaphrodite gonad size and shape by vab-3/Pax6-mediated regulation of integrin receptors. Genes Dev. 2007; 21:1615–1620. [PubMed: 17606640]

Merz DC, Zheng H, Killeen MT, Krizus A, Culotti JG. Multiple signaling mechanisms of the UNC-6/netrin receptors UNC-5 and UNC-40/DCC in vivo. Genetics. 2001; 158:1071–1080. [PubMed: 11454756]

Nishiwaki K. Mutations affecting symmetrical migration of distal tip cells in *Caenorhabditis elegans*. Genetics. 1999; 152:985–997. [PubMed: 10388818]

Pfaff M, Liu S, Erle DJ, Ginsberg MH. Integrin beta cytoplasmic domains differentially bind to cytoskeletal proteins. J Biol Chem. 1998; 273:6104–6109. [PubMed: 9497328]

Playford MP, Schaller MD. The interplay between Src and integrins in normal and tumor biology. Oncogene. 2004; 23:7928–7946. [PubMed: 15489911]

Poinat P, De Arcangelis A, Sookhareea S, Zhu X, Hedgecock EM, Labouesse M, Georges-Labouesse E. A conserved interaction between beta1 integrin/PAT-3 and Nck-interacting kinase/MIG-15 that mediates commissural axon navigation in *C. elegans*. Curr Biol. 2002; 12:622–631. [PubMed: 11967148]

Reddien PW, Horvitz HR. CED-2/CrkII and CED-10/Rac control phagocytosis and cell migration in *Caenorhabditis elegans*. Nat Cell Biol. 2000; 2:131–136. [PubMed: 10707082]

Schmidt KL, Marcus-Gueret N, Adeleye A, Webber J, Baillie D, Stringham EG. The cell migration molecule UNC-53/NAV2 is linked to the ARP2/3 complex by ABI-1. Development. 2009; 136:563–574. [PubMed: 19168673]

Serafini T, Kennedy TE, Galko MJ, Mirzayan C, Jessell TM, Tessier-Lavigne M. The netrins define a family of axon outgrowth-promoting proteins homologous to *C. elegans* UNC-6. Cell. 1994; 78:409–424. [PubMed: 8062384]

Shakir MA, Gill JS, Lundquist EA. Interactions of UNC-34 Enabled with Rac GTPases and the NIK kinase MIG-15 in *Caenorhabditis elegans* axon pathfinding and neuronal migration. Genetics. 2006; 172:893–913. [PubMed: 16204220]

Shattil SJ, Kim C, Ginsberg MH. The final steps of integrin activation: the end game. Nat Rev Mol Cell Biol. 2010; 11:288–300. [PubMed: 20308986]

Siegfried KR, Kidd AR 3rd, Chesney MA, Kimble J. The sys-1 and sys-3 genes cooperate with Wnt signaling to establish the proximal-distal axis of the *Caenorhabditis elegans* gonad. Genetics. 2004; 166:171–186. [PubMed: 15020416]

Simmer F, Moorman C, van der Linden AM, Kuijk E, van den Berghe PV, Kamath RS, Fraser AG, Ahringer J, Plasterk RH. Genome-wide RNAi of *C. elegans* using the hypersensitive rrf-3 strain reveals novel gene functions. PLoS Biol. 2003; 1:E12. [PubMed: 14551910]

Tadokoro S, Shattil SJ, Eto K, Tai V, Liddington RC, de Pereda JM, Ginsberg MH, Calderwood DA. Talin binding to integrin beta tails: a final common step in integrin activation. Science. 2003; 302:103–106. [PubMed: 14526080]

Timmons L. Delivery methods for RNA interference in *C. elegans*. Methods Mol Biol. 2006; 351:119–125. [PubMed: 16988430]

Wadsworth WG, Bhatt H, Hedgecock EM. Neuroglia and pioneer neurons express UNC-6 to provide global and local netrin cues for guiding migrations in *C. elegans*. Neuron. 1996; 16:35–46. [PubMed: 8562088]

Wegener KL, Partridge AW, Han J, Pickford AR, Liddington RC, Ginsberg MH, Campbell ID. Structural basis of integrin activation by talin. Cell. 2007; 128:171–182. [PubMed: 17218263]

Wu YC, Horvitz HR. *C. elegans* phagocytosis and cell-migration protein CED-5 is similar to human DOCK180. Nature. 1998; 392:501–504. [PubMed: 9548255]

Xu X, Rongali SC, Miles JP, Lee KD, Lee M. pat-4/ILK and unc-112/Mig-2 are required for gonad function in *Caenorhabditis elegans*. Exp Cell Res. 2006; 312:1475–1483. [PubMed: 16476426]

Yigit E, Batista PJ, Bei Y, Pang KM, Chen CC, Tolia NH, Joshua-Tor L, Mitani S, Simard MJ, Mello CC. Analysis of the *C. elegans* Argonaute family reveals that distinct Argonautes act sequentially during RNAi. Cell. 2006; 127:747–757. [PubMed: 17110334]

Zhang Y, Chen D, Smith MA, Zhang B, Pan X. Selection of reliable reference genes in *Caenorhabditis elegans* for analysis of nanotoxicity. PLoS One. 2012; 7:e31849. [PubMed: 22438870]

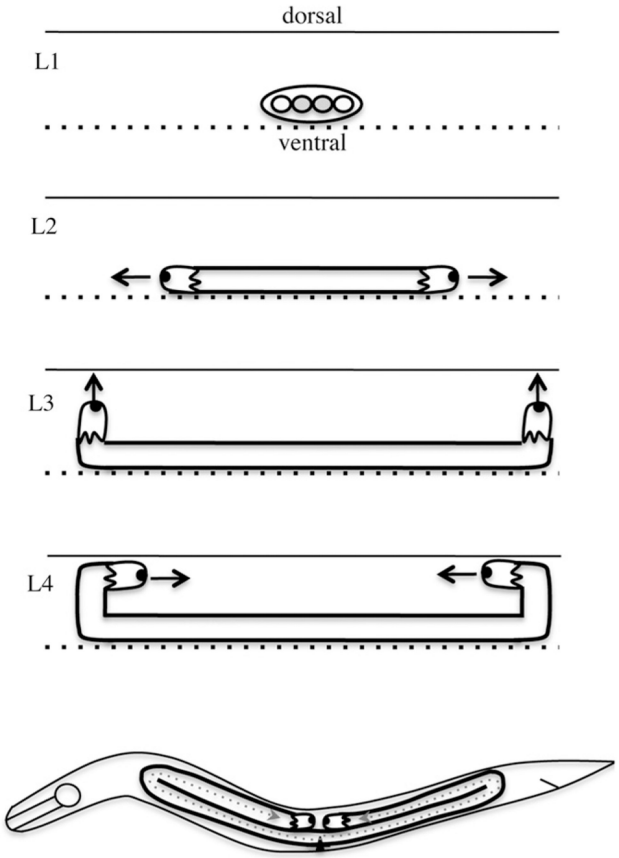

Fig. 1.

DTC migration path determines the shape of the hermaphrodite gonad arms. DTCs are born in the first larval stage (L1) from the somatic gonad precursors Z1 and Z4 (white circles) in the gonad primordium with the germ cell precursors Z2 and Z3 (grey circles). DTCs commence migration during the second larval stage (L2) and travel in opposite directions along the ventral basement membrane (dotted lines). In the middle of the third larval stage (L3), DTCs reorient on ventral and migrate toward the dorsal side (solid lines), where they turn again, and in the fourth larval stage (L4) they migrate toward one another along the dorsal surface. The entire path is complete by the end of the fourth larval stage. The bottom schematic places the gonad arms within the body of the animal. Grey dashed arrows trace opposite paths. The black triangle indicates the vulva located at the midbody.

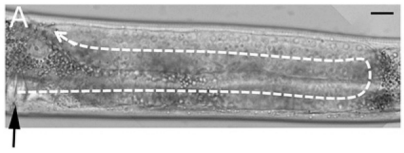

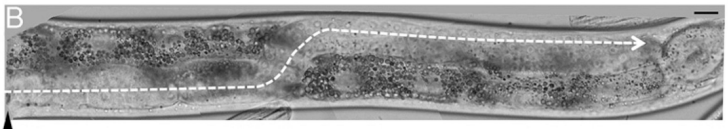

C

Genotype/ RNAi	wild-type (%)	wrong turn on dorsal (%)	extended linear (%)	N
rrf-3(pk1426)/ empty	100	0	0	>300
rrf-3(pk1426)/ mig-38	35 ± 8	59 ± 8	6 ± 4	145
rrf-3(pk1426)/ mig-38^{IS1} + mig-38^{IS2}	68 ± 9	32 ± 9	0	100
rde-1(ne219); lag-2p::RDE-1/ *empty*	91 ± 5	9 ± 5	0	105
rde-1(ne219); lag-2p::RDE-1/ *mig-38*	66 ± 8	34 ± 8	0	122

Fig. 2.

Cell-autonomous effects of *mig-38* RNAi on DTC turning. *rrf-3*(*pk1426*) hermaphrodites were grown on *E. coli* HT115(DE3) either carrying pPD129.36 without an insert (*empty*) (A and C) or pPD129.36-*mig-38* plasmid (*mig-38*) (B and C). White dashed arrows trace the migration paths of the DTCs. The black arrows point to the vulva. In all panels, dorsal side is up. Scale bar: 10 μm. (C) Quantification of gonad malformations with various RNAi treatments. Hermaphrodites of specific genotype were fed with bacteria carrying pPD129.36 with inserts targeting different parts of the *mig-38* transcript: *mig-38*, *mig-38^{IS1}* and *mig-38^{IS2}* (described in the Materials and Methods), or with empty vector. Turning defects were assessed in the late L4/young adult stage of hermaphrodites subjected to RNAi. Gonad shapes are drawn at the top of each column. Phenotypes are described in the Materials and Methods. *N*=the number of gonad arms. Standard errors were calculated using the observed frequency and the actual sample size, assuming a normal binomial distribution. The overall percentage of defects induced by knockdown of *mig-38* in *rde-1*(*ne219*); *lag-2p*::RDE-1 is lower than in the *rrf-3*(*pk1426*) strain, because *rrf-3*(*pk1426*) is sensitized to RNAi.

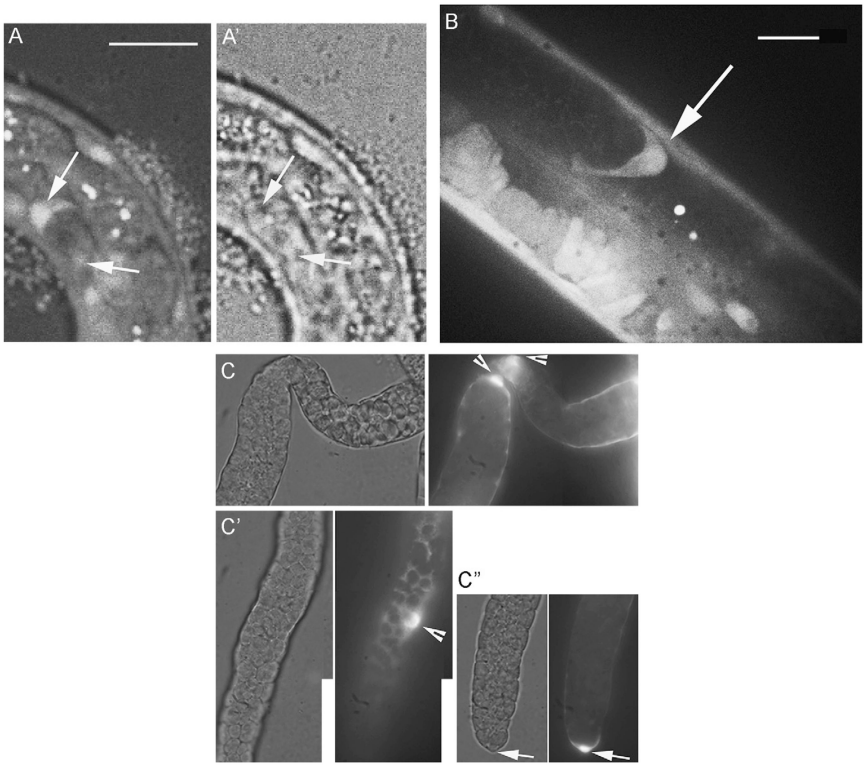

Fig. 3.

mig-38 is expressed in DTCs and gonadal sheath cells. (A) DIC image of an L1 hermaphrodite expressing *F40F11.2/mig-38*p::GFP merged with the confocal image in the same focal plane. (A′) DIC image highlighting the gonad primordium. White arrows point to Z1 and Z4 DTC precursor cells in the gonad primordium. Scale bar: 10 μm. (B) Confocal image of an L4 stage hermaphrodite. White arrow points to the DTC. Scale bar: 10 μm. (C and C″) Matching pairs of DIC (left) and fluorescence (right) images representing different parts of the same dissected gonad arm of a young adult *mig-38*p::GFP hermaphrodite: fluorescence shows a GFP-positive sheath cell nuclei at the juncture of proximal and distal sections of the gonad arm (C) and in the distal gonad (C′), and GFP in the DTC in images focused on the tip of the distal gonad (C″). Arrowheads point to gonadal sheath cell nuclei containing GFP. White arrows point to the DTC.

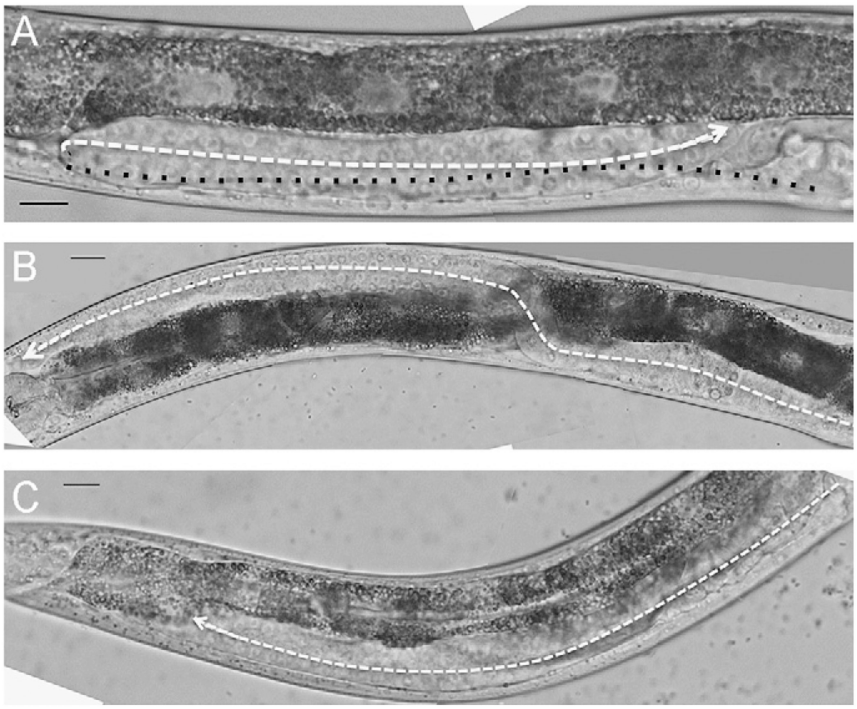

Fig. 4.

Knockdown of *mig-38* expression affects turning on the ventral side. Dashed lines trace the DTC paths in DIC images of gonad arms in hermaphrodites at late L4/young adult stage. Dorsal side is up. (A) *unc-6* (*ev400*) hermaphrodite posterior gonad; black dotted line traces the proximal gonad and white dashed line traces the distal gonad on top of it. Both are on the ventral side. (B) N2 hermaphrodite subjected to *mig-38* RNAi; anterior gonad shows the wrong turn on dorsal phenotype. (C) *unc-6*(*ev400*) hermaphrodite subjected to *mig-38* RNAi; posterior gonad does not turn but remains on the ventral side for the entire path. Scale bars: 10 μm.

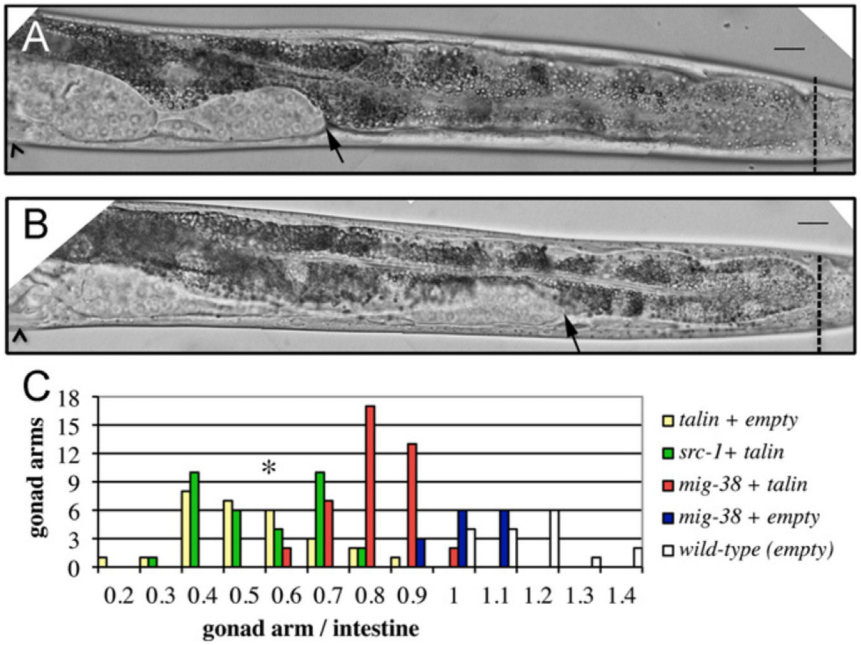

Fig. 5.

mig-38 RNAi suppresses the premature stop phenotype of DTCs with *talin* RNAi. DIC images of late L4 hermaphrodites show gonad arm morphologies from treatment with *talin*, *empty* RNAi (A) or *talin, mig-38* RNAi (B). Black arrows mark the DTCs, arrowheads indicate the vulvas, and dotted lines show the end of the intestines. Scale bars: 10 μm. (C) The graph shows the relative sizes of gonad arms with different treatments. The length of the gonad arm (from the vulva to the end of the gonad) was divided by the length of the intestine (from the vulva to the end of the intestine) in late L4/young adult *rrf-3*(*pk1426*) treated by feeding RNAi with *talin*+*empty* (yellow), *talin*+*mig-38* (red), *mig-38*+*empty* (blue), *talin*+*src-1* (green), and empty vector (wild-type, white). The asterisk indicates the average relative size at the turning point for a wild type gonad arm in late L4/young adult *rrf-3*(*pk1426*) hermaphrodites.

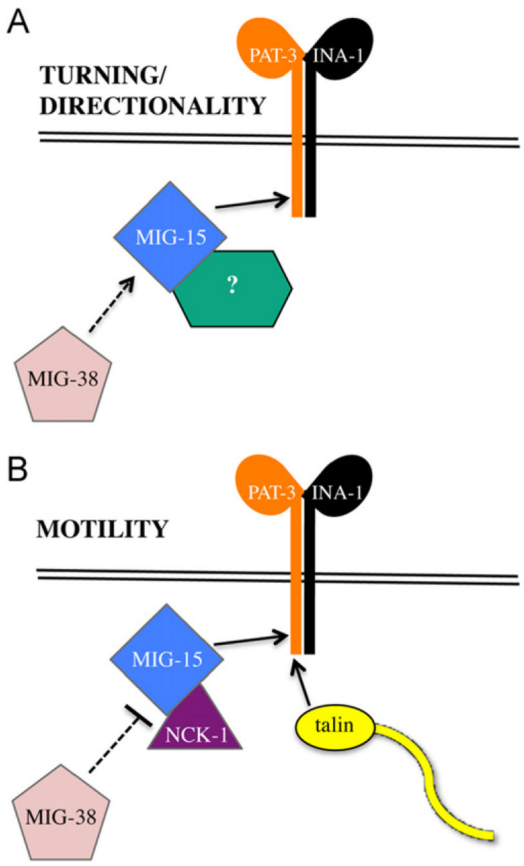

Fig. 6.

Model for the role of MIG-38 in DTC turning. The integrin heterodimer INA-1/PAT-3 is required for motility and turning of the DTCs and its activity is regulated by two associated proteins, talin and MIG-15. (A) Downregulation of MIG-38 with either MIG-15 or INA-1 exacerbates defects in turning, placing it in a role as a potentiator of a turning pathway mediated by *mig-15* and *ina-1*. MIG-38 may promote MIG-15 interactions with binding partners that induce INA-1/PAT-3 functions in changing the direction of migration. (B) Talin promotes integrin-mediated motility. MIG-38 downregulation relieves the motility defect that results from knockdown of talin. Depletion of both MIG-38 and talin uncovers a role for MIG-15 and its binding partner NCK-1, indicating that a MIG-15/NCK-1 complex plays a role in DTC motility.

Table 1

Quantification of *mig-38* RNAi-induced DTC turning defects.

Genotype/treatment	Wild-type (%)	Ventralized (%)	Wrong turn on dorsal (%)	Extended linear (%)	Other (%)	*N*
Wild-type (N2)	100	0	0	0	0	170
Netrin						
N2/mig-38	86 ± 4	0	14 ± 4	0	0	270
unc-6(ev400)/empty	29 ± 7	66 ± 8	0	5 ± 4	0	149
unc-6(ev400)/mig-38	11.5 ± 4	26 ± 6	0.5 ± 1	62 ± 7	0	206
Integrin						
rrf-3(pk1426)	100	0	0	0	0	> 300
rrf-3(pk1426)/mig-38+e	56 ± 5	0	38 ± 5	6 ± 3	0	339
rrf-3(pk1426)/ina-1+e	75 ± 7	4.5 ± 4	7.5 ± 4	7 ± 4	6 ± 4	132
rrf-3(pk1426) ina-1+mig-38	31 ± 7	1 ± 2	24 ± 7	34 ± 8	10 ± 5	152

Defects were assessed in the late L4/young adult stage of hermaphrodites subjected to RNAi. *N*=the number of gonad arms. All phenotypes are described in the Materials and Methods. Wild-type, wrong turn on dorsal, and extended linear gonad phenotypes are illustrated in Fig. 2C. In ventralized gonads, the DTCs turn back to the midbody on the ventral side.

Dev Biol. Author manuscript; available in PMC 2013 August 15.

Table 2

mig-38 and *mig-15* act together to regulate turning.

Genotype/RNAi	Wild-type (%)	Wrong turn on dorsal (%)	Extended (%)	Other (%)	*N*
rrf-3(*pk1426*)	100	0	0	0	> 300
rrf-3(*pk1426*)*/mig-38*+*2* × *empty*	70 ± 5	30 ± 5	0	0	278
rrf-3(*pk1426*)*/mig-15*+*2* × *empty*	92 ± 4	8 ± 4	0	0	146
rrf-3(*pk1426*)*/mig-38*+*mig*-15+*e*	50 ± 7	46 ± 7	3 ± 3	1 ± 1	178
mig-15(*rh80*)	93 ± 4	3 ± 3	3 ± 2	1 ± 2	156
mig-15(*rh80*)*/mig-38*	50 ± 14	15 ± 10	33 ± 13	2 ± 4	52
Wild-type (*N2*)	100	0	0	0	170
N2/mig-38	86 ± 4	14 ± 4	0	0	270

Defects were assessed in the late L4/young adult stage of hermaphrodites subjected to RNAi. *N* = the number of gonad arms. All phenotypes are described in the Materials and Methods.

Table 3

mig-38 RNAi suppresses migration defect of *talin* RNAi.

Genotype/RNAi	Wild-type (%)	Short (%)	Turn (%)[a]	*N*
rrf-3(*pk1426*)	100	0	0	> 300
rrf-3(*pk1426*)/*mig-38*+*empty*	56 ± 5	0	44 ± 5	339
rrf-3(*pk1426*)/*src-1* +*empty*	63 ± 9	0	37 ± 9	102
rrf-3(*pk1426*)/*talin*+ *empty*	19 ± 5	44 ± 7	37 ± 6	219
rrf-3(*pk1426*)/*talin*+ *mig-38*	18 ± 6	0	82 ± 6	165
rrf-3(*pk1426*)/*talin*+ *src-1*	16 ± 7	42 ± 9	42 ± 79	104

Defects were assessed in the late L4/young adult stage of hermaphrodites subjected to RNAi. *N* = the number of gonad arms. All phenotypes are described in the Materials and Methods.

[a]Turn defects include wrong turn on dorsal and extended linear gonad arms. Ventralized gonad arms and other defects in gonad morphology constituted less that 5% of defects and were not included in the analysis.

Table 4

Effects of *mig-15* or *nck-1* RNAi on *mig-38* and *talin* RNAi defects.

Genotype/RNAi	Wild-type (%)	Short (%)	Turn (%)[a]	*N*
rrf-3(pk1426)/talin+2 × empty	18 ± 4	51.5 ± 5	30.5 ± 5	304
rrf-3(pk1426)/mig-38 + talin+ empty	20.3 ± 5	5.4 ± 3	74.3 ± 5	280
rrf-3(pk1426)/mig-38+2 × empty	70 ± 5	0	30 ± 5	278
rrf-3(pk1426)/mig-15+2 × empty	92 ± 4	0	8 ± 4	146
rrf-3(pk1426)/mig-15 + talin+ empty	21 ± 8	58 ± 10	21 ± 8	150
rrf-3(pk1426)/mig-15 + mig-38+ talin	6 ± 4	22 ± 6	72 ± 7	173
N2/mig-38+ empty	88 ± 9	0	12 ± 9	52
N2/talin+ empty	70 ± 7	5 ± 3	25 ± 7	152
mig-15(rh80)	93 ± 4	1 ± 2	6 ± 3	156
mig-15(rh80)/mig-38+ empty	62 ± 8	0	38 ± 8	132
mig-15(rh80)/talin+ empty	44 ± 8	28 ± 7	28 ± 7	141
mig-15(rh80)/mig-38+ talin	25 ± 7	20 ± 7	55 ± 8	144
rrf-3(pk1426)/pat-4+2 × empty	9773	0	373	102
rrf-3(pk1426)/pat-4+ mig-38+ empty	68 ± 9	0	32 ± 9	100
rrf-3(pk1426)/pat-4 + talin+ empty	18 ± 8	46 ± 10	36 ± 10	92
rrf-3(pk1426)/pat-4+ mig-38+ talin	28 ± 9	4 ± 4	68 ± 9	99
rrf-3(pk1426)/nck-1 +2 × empty	100	0	0	100
rrf-3(pk1426)/nck-1 + mig-38+ empty	74 ± 8	0	26 ± 8	106
rrf-3(pk1426)/nck-1 + talin+ empty	9 ± 6	63 ± 9	28 ± 9	100
rrf-3(pk1426)/nck-1 + mig-38+ talin	12 ± 6	20 ± 7	68 ± 9	112

Defects were assessed in the late L4/young adult stage of hermaphrodites subjected to RNAi. *N*=the number of gonad arms. All phenotypes are described in the Materials and Methods.

[a]Turn defects include wrong turn on dorsal, extended linear gonad arms, and extra turns. Extra turns represent fewer than 1% of defects in all treatments with the exception of *pat-4* RNAi where as many as 6% of the turning defects were extra turns. Ventralized gonad arms constituted less than 5% of total defects and were not included in the analysis.